Inorg. Chem. **2006**, *45*, 10329–10337

Role of Donor and Secondary Interactions in the Structures and Thermal Properties of Alkaline-Earth and Rare-Earth Metal Pyrazolates

Julia Hitzbleck,[†,‡] Anna Y. O'Brien,[†] Glen B. Deacon,*[,‡] and Karin Ruhlandt-Senge*[,†,‡]

Department of Chemistry, Syracuse University, Syracuse, New York 13244-4100, and School of Chemistry, Monash University, Clayton, Victoria 3168, Australia

Received July 13, 2006

The addition of neutral coligands to reduce the aggregation and improve the volatility of potential heavy alkaline-earth metal chemical vapor deposition (CVD) precursors has typically resulted in liberation of the coligand upon heating. A new series of dinuclear alkaline-earth and rare-earth metal pyrazolates, bis[bis(3,5-di-*tert*-butylpyrazolato)-(tetrahydrofuran)calcium] (**1**), bis[bis(3,5-di-*tert*-butylpyrazolato)(tetrahydrofuran)strontium] (**2**), and bis[bis(3,5-di-*tert*-butylpyrazolato)bis(tetrahydrofuran)barium] (**3**), have been obtained from our previous donor-free oligonuclear complexes $[\{M(3,5\text{-}t\text{Bu}_2\text{pz})_2\}_n]$ (**5**, M = Ca, $n = 3$; **6**, M = Sr, $n = 4$; **7**, M = Ba, $n = 6$) by treatment with tetrahydrofuran (THF). Compounds **1**–**3**, as well as the europium analogue bis[bis(3,5-di-*tert*-butylpyrazolato)-(tetrahydrofuran)europium(II)] (**4**), can also be prepared by direct reaction of the metals and pyrazole in THF and anhydrous liquid ammonia. Recrystallization from hexane led to single crystals of **2**–**4**, while the powder diffraction pattern of **1** revealed it to be isostructural with the previously published bis[bis(3,5-di-*tert*-butylpyrazolato)-(tetrahydrofuran)ytterbium(II)] (**8**), providing important insight into differences and similarities between the two groups of metals. Detailed structural analysis of the compounds reveals secondary interactions including π-bonding and agostic interactions, which are considered essential in stabilizing the metal complexes. The direct comparison of structural features and thermal properties (as evaluated by thermogravimetric analysis and sublimation studies) of the donor-free oligonuclear and the donor-containing dinuclear species offers a better understanding of the role of donors and secondary interactions.

Introduction

The interest in Group 2 complexes for advanced electronic materials was initiated by the development of the $YBa_2Cu_3O_{7-x}$ high-temperature superconductors[1] and has been growing ever since.[2] Numerous other multicomponent electroceramic materials such as high-permittivity dielectric $Ba_xSr_{1-x}TiO_3$ for next-generation dynamic random access memory and $SrBi_2Ta_2O_9$ for thin film ferroelectric nonvolatile memories contain heavy alkaline-earth metals.[3] A number of oxygen-free materials, including the sulfide phosphors SrS:Ce/SrS:Cu for thin film electroluminescent displays, and Group 2 doped III−V semiconductors have also found widespread use.[4] The rapid improvements in computer technology along with the quest for even faster and smaller electronic devices requires a uniform, high-purity deposition of thin films, produced by chemical vapor deposition (CVD) processes. Even though progress has been made toward alternative film growth methods (atomic layer deposition, liquid delivery metal−organic, and supercritical fluid transport),[5] CVD remains the most desired technology, and the quest for volatile precursor molecules with sufficient thermal stability remains. A variety of such compounds have appeared in the

* To whom correspondence should be addressed. E-mail: Glen.Deacon@sci.monash.edu.au (G.B.D.), kruhland@syr.edu (K.R.-S.). Phone: (+61)3-9905-4568 (G.B.D.), (+1)315-443-1306 (K.R.-S.). Fax: (+61)3-9905-4597 (G.B.D.), (+1)315-443-4070 (K.R.-S.).

† Syracuse University.

‡ Monash University.

(1) (a) Bednorz, J. G.; Mueller, K. A. *Z. Phys. B: Condens. Matter* **1986**, *64*, 189. (b) Geballe, T. H.; Hulm, J. K. *Science* **1988**, *239*, 367. (c) Horowitz, H. S.; McLain, S. J.; Sleight, A. W.; Druliner, J. D.; Gai, P. L.; Vankavelaar, M. J.; Wagner, J. L.; Biggs, B. D.; Poon, S. J. *Science* **1989**, *243*, 66.

(2) (a) Gordon, R. G.; Barry, S. T.; Liu, X.; Teff, D. J. *Mater. Res. Soc. Symp. Proc.* **1999**, *574*, 23. (b) Otway, D. J.; Rees, W. S., Jr. *Coord. Chem. Rev.* **2000**, *210*, 279.

(3) (a) Barron, A. R.; Rees, W. S., Jr. *Adv. Mater. Opt. Electron.* **1993**, *2*, 271. (b) Gordon, R. G.; Barry, S.; Broomhall-Dillard, R. N. R.; Teff, D. J. *Adv. Mater. Opt. Electron.* **2000**, *10*, 201.

(4) (a) Yuta, M. M.; White, W. B. *J. Electrochem. Soc.* **1992**, *139*, 2347. (b) Lowe-Ma, C. K.; Vanderah, T. A.; Smith, T. E. *J. Solid State Chem.* **1995**, *117*, 363.

(5) Matthews, J. S.; Rees, W. S., Jr. *Adv. Inorg. Chem.* **2000**, *50*, 173.

10.1021/ic061294d CCC: $33.50
Published on Web 11/09/2006

literature, but only a few show potential for use in oxide-free materials; problems are often encountered in the film growth because of unacceptable high-impurity incorporation (C, F, and O) and low vapor pressure.[6]

It is particularly challenging to obtain volatile complexes for the heavier alkaline-earth metals because of their low charge/size ratio, and thus a high tendency to form aggregated, nonvolatile, oligonuclear structures. A common remedy to avoid aggregation is to incorporate neutral coligands to saturate the coordination sphere of the metal, thereby reducing the nuclearity of the compound. However, loss of these dative ligands upon heating frequently results in aggregation and poor thermal stability of alkaline-earth metal β-diketonate and β-ketiminate precursors for example, and even complexes with tethered "lariat" donor functionalities showed only poor thermal stability.[7] Recently, the same problem has been noted for alkaline-earth metal pyrazolate complexes synthesized for use as CVD precursors.[8] Work by Winter et al. has shown the loss of tetrahydrofuran (THF), polyamine, or polyether donors (D) from pyrazolate complexes of the type $[M(t\mathrm{Bu_2pz})_2(D)_n]$ (M = Mg, Ca, Sr, Ba).[8] These compounds decompose upon sublimation, with formation of $t\mathrm{Bu_2pzH}$ and a nonvolatile aggregate $[\{Ca(t\mathrm{Bu_2pz})_2\}_n]$, recently shown to be trinuclear $[\{Ca(t\mathrm{Bu_2pz})_2\}_3]$.[9] The only exception noted in this series was the complex $[Ca(t\mathrm{Bu_2pz})_2(\text{triglyme})]$, which sublimed in moderate yield, attributable to an increased thermal stability resulting from a good steric "fit" of this donor.[8]

Comparative studies have shown striking similarities between calcium and strontium and the divalent lanthanoids samarium, yttrium, and europium because of very similar, low charge/size ratios. As such, the successful doping of gallium arsenide films with erbium by metal−organic vapor-phase epitaxy (MOVPE) using $[Er(t\mathrm{Bu_2pz})_3(4\text{-}tert\text{-butylpyridine})_2]$ is noteable, although the trivalent erbium displays a slightly smaller ionic radius and higher charge/size ratio.[10]

Despite some earlier results indicating limited thermal stability of alkaline-earth metal pyrazolates, the promising results presented for the trivalent erbium and calcium triglyme adduct motivated us to further investigate the $t\mathrm{Bu_2}$-pz ligand in conjunction with the alkaline-earth metals. We were specifically interested in further investigating the factors involved in donor liberation, as presented here with a family of alkaline-earth metal di-*tert*-butylpyrazolates that exist in both a donor-containing dinuclear form (compounds **1**−**3**) and a donor-free oligonuclear form (compounds **5**−**7**).[9] The donor-containing europium analogue (**4**) is also presented.

Scheme 1. Solvation of Compounds **1**, **1a**, **2**, **3**, and **5**−**7**[a]

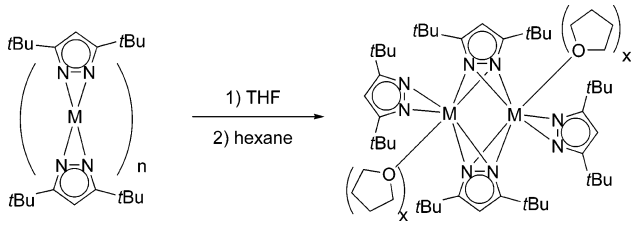

[a] M = Ca, $n = 3$, $x = 1$ (**1a**), 2 (**1**); M = Sr, $n = 4$, $x = 1$ (**2**); M = Ba, $n = 6$, **2**; M = Ba, $x = 2$ (**3**).

The pyrazolate ligand has been pursued as a non-oxygen-containing alternative to the β-diketonate ligands. Advantages include (i) a robust core with various substitution sites and a large number of possible substituents to tailor the steric demand of the ligand, (ii) the option of good solubility achieved without introduction of silicon- and fluorine-containing substituents, and (iii) the high basicity of the aromatic heterocycle to provide a strong binding potential, leading to better gas-phase stability of the compounds. Previous methods to prepare the pyrazolate target compounds include salt metathesis and transamination pathways,[6b,9,11] both two-step procedures. Here, we report on direct metalation as an inexpensive, facile, one-step alternative.[9,11]

Our recently prepared monomeric 3,5-diphenylpyrazolates $[M(\eta^2\text{-}\mathrm{Ph_2pz})_2(THF)_4]$ (M = Ca, Sr, Ba; **9a**−**c**) and $[M(\mathrm{Ph_2pz})_2(DME)_m]$ (M = Ca, Sr, $m = 2$; M = Ba, $m = 3$; **9d**−**f**)[11] were not volatile, and in the absence of coligands, these compounds displayed very poor solubility, consistent with oligonuclear structures. In an effort to address the problem of neutral coligand liberation upon heating, we here report on the heteroleptic compounds $[\{M(t\mathrm{Bu_2pz})_2(THF)_x\}_2]$ ($x =$ 1, M = Ca, **1**; Sr, **2**; Eu, **4**; $x = 2$, M = Ba, **3**) obtained by exposure of the homoleptic, linear, oligonuclear **5**−**7** to THF, as well as by direct synthesis from the free metals. This work allows for the first time the direct comparison of cosolvent-containing and -free alkaline-earth pyrazolates, thus providing new insights into the debilitating process of donor loss and subsequent lowered volatility.

Results and Discussion

Preparation of 3,5-Di-*tert*-butylpyrazolate Complexes. Dissolution of compounds **5**−**7** in THF (Scheme 1) led to the formation of heteroleptic complexes of composition $[\{M(t\mathrm{Bu_2pz})_2(THF)_x\}_n]$ (M = Ca, $x = 2$, $n = 1$, **1a**; M = Sr, $x = 1$, $n = 2$, **2**; M = Ba, $x = 2$, $n = 2$, **3**) by ^{1}H NMR spectroscopy in benzene-d_6. The formation of the crude product $[Ca(t\mathrm{Bu_2pz})_2(THF)_2]$ (**1a**) confirms a previous report of a thermally unstable monomeric complex,[8b] but **1a** loses 1 equiv of THF upon recrystallization from hexane to give **1**. As reported for the related ytterbium complex $[\{Yb(t\mathrm{Bu_2}$-

(6) (a) Wojtczak, W. A.; Fleig, P. F.; Hampden-Smith, M. J. *Adv. Organomet. Chem.* **1996**, *40*, 215. (b) Otway, D. J.; Rees, W. S., Jr. *Coord. Chem. Rev.* **2000**, *210*, 279. (c) Hanusa, T. P. *Organometallics* **2002**, *21*, 2559.
(7) Studebaker, D. B.; Neumayer, D. A.; Hinds, B. J.; Stern, C. L.; Marks, T. J. *Inorg. Chem.* **2000**, *39*, 3148.
(8) (a) Pfeiffer, D.; Heeg, M. J.; Winter, C. H. *Angew. Chem., Int. Ed.* **1998**, *37*, 2517; *Angew. Chem.* **1998**, *110*, 2674. (b) Pfeiffer, D.; Heeg, M. J.; Winter, C. H. *Inorg. Chem.* **2000**, *39*, 2377. (c) El-Kaderi, H. M.; Heeg, M. J.; Winter, C. H. *Polyhedron* **2005**, *24*, 645.
(9) Hitzbleck, J.; Deacon, G. B.; Ruhlandt-Senge, K. *Angew. Chem., Int. Ed.* **2004**, *43*, 5218; *Angew. Chem.* **2004**, *116*, 5330.
(10) (a) Cederberg, J. G.; Culp, T. D.; Bieg, B.; Pfeiffer, D.; Winter, C. H.; Bray, K. L.; Kuech, T. F. *J. Cryst. Growth* **1998**, *195*, 105. (b) Cederberg, J. G.; Culp, T. D.; Bieg, B.; Pfeiffer, D.; Winter, C. H.; Bray, K. L.; Kuech, T. F. *J. Appl. Phys.* **1999**, *85* (3), 1825. (c) Pfeiffer, D.; Ximba, B. J.; Liable-Sands, L. M.; Rheingold, A. L.; Heeg, M. J.; Coleman, D. M.; Schlegel, H. B.; Kuech, T. F.; Winter, C. H. *Inorg. Chem.* **1999**, *38*, 4539.
(11) Hitzbleck, J.; O'Brien, A. Y.; Deacon, G. B.; Ruhlandt-Senge, K. *Chem.—Eur. J.* **2004**, *10*, 3315.

Scheme 2. Synthesis of Compounds **1**−**4** from the Metals[a]

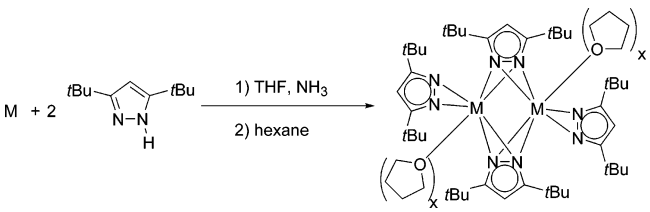

[a] M = Ca, $x = 1$, **1**; M = Sr, $x = 1$, **2**; M = Ba, $x = 2$, **3**; M = Eu, $x = 1$, **4**.

$pz)_2(THF)\}_2]$ (**8**),[12] recrystallization from a hydrocarbon solvent and subsequent loss of one THF donor from **1a** seems to be a crucial step toward the isolation of **1**, inducing dimerization to achieve coordinative saturation.

The target complexes were also prepared by direct metalation using liquid ammonia activated metals (Scheme 2). Stoichiometric amounts of metal and 3,5-di-*tert*-butylpyrazole were reacted in THF/NH_3 followed by recrystallization of the crude material from hexane (**1**, **2**, and **4**; hexane/THF for **3**) to afford the crystalline products $[\{M(t\mathrm{Bu}_2pz)_2(THF)_x\}_2]$ (M = Ca, $x = 1$, **1**; M = Sr, $x = 1$, **2**; M = Ba, $x = 2$, **3**; M = Eu, $x = 1$, **4**) in good yield and purity.

The spectroscopic and analytical data are in agreement with the molecular structures determined by X-ray crystallography; compound **3** contains one lattice THF molecule, which was removed during refinement because of unresolvable disorder. Low-temperature ^{1}H NMR spectra of **1**−**3** in toluene-d_8 show complex changes upon cooling/warming involving splitting of the C4(pz)−H and *t*Bu signal, consistent with the different environments of terminal and bridging ligands. However, no clean separation into two well-defined C4(pz)−H peaks of equal integration at the lowest temperature (193 K) is observed (see the Supporting Information). The IR spectra of **1**−**4** are essentially identical, and electrospray ionization mass spectrometry (ESIMS) data of acetonitrile (MeCN) solutions of **1** show the corresponding signals of MeCN-solvated fragments. Elemental analysis gave satisfactory results for **2** and **4** and indicated substantial loss of 4THF/dinuclear arrangment for **3**. The identity of **1** was confirmed by a well-resolved powder pattern, representing a perfect match with the calculated powder pattern from single-crystal data for the ytterbium complex **8**.[12] The absence of additional peaks indicated the purity of the sample. The similar structural patterns of **1** and **8** are not surprising considering the similar sizes of Yb^{2+} and Ca^{2+},[13] an observation also seen previously with regards to structural and spectroscopic features of alkaline-earth and divalent rare-earth metal pyrazolates.[9,12]

Molecular Structure of 1 and Crystal Structures of 2−**4.** Recrystallization of **1** repeatedly resulted in white, soft crystals of insufficient quality for single-crystal X-ray diffraction; therefore, the solid material was subjected to X-ray powder diffraction studies. Refinement of the unit cell parameters indicated that **1** is isostructural with the ytterbium analogue **8**.[12] Single crystals were obtained for compounds

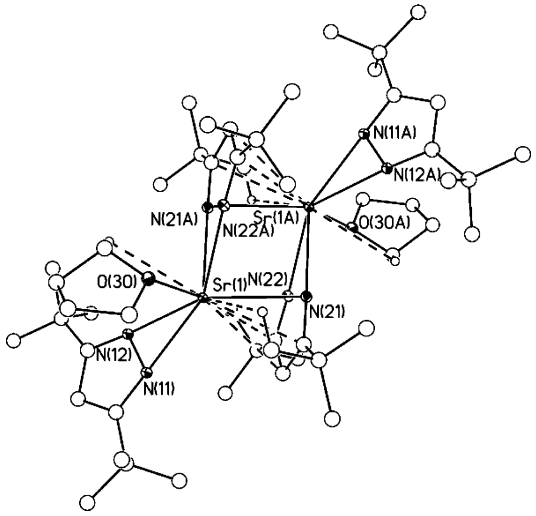

Figure 1. Computer-generated plot of **2** with thermal ellipsoids depicting 50% probability. Dotted lines symbolize additional bonding interactions. The hydrogen atoms {except for CH_3 [C(253)] and CH_2 [(C(31)] involved in agostic interactions} have been omitted for clarity.

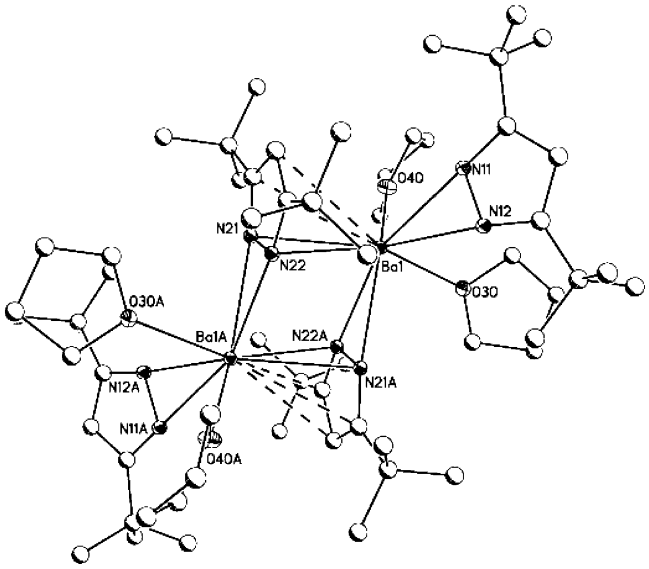

Figure 2. Perspective view of **3** with anisotropic displacement parameters depicting 50% probability. Dotted lines symbolize additional bonding interactions. The hydrogen atoms have been omitted for clarity.

2−**4,** and their analysis by X-ray diffraction techniques allowed the determination of their respective molecular geometries; the crystal structures of **5**−**7** were communicated previously.[9] Representative views of compounds **2** and **3** are shown in Figures 1 and 2, respectively. Experimental crystallographic data are summarized in Table 1; pertinent bond lengths and angles are listed in Table 2. Observed and calculated structure factor details are available from the authors upon request. CCDC 283705−283707 (**2**−**4**) contain the supplementary crystallographic data for this paper. These data can be obtained free of charge at www.ccdc.cam.ac.uk/conts/retrieving.html [or from the Cambridge Crystallographic Data Centre, 12 Union Road, Cambridge CB2 1EZ, U.K.; fax (international) +44-1223/336-033; e-mail deposit@ccdc.cam.ac.uk].

Complexes **2** and **4** are isostructural and exist as centrosymmetric dinuclear units bridged by chelating μ-η^2:η^5-

(12) Deacon, G. B.; Delbridge, E. E.; Skelton, B. W.; White, A. H. *Angew. Chem., Int. Ed.* **1998**, *37*, 2251; *Angew. Chem.* **1998**, *110*, 2372.
(13) Shannon, R. D. *Acta Crystallogr., Sect. A* **1976**, *32* (5), 751.

Table 1. Crystallographic Data for Compounds **1**−**4**

	1[a]	**2**	**3**	**4**
chemical formula	$C_{52}H_{92}Ca_2N_8O_2$	$C_{52}H_{92}N_8O_2Sr_2$	$C_{60}H_{108}Ba_2N_8O_4$	$C_{52}H_{92}Eu_2N_8O_2$
fw	941.496	1036.58	1280.20	1165.28
space group	$P\bar{1}$ (No. 2)	$P\bar{1}$ (No. 2)	$P\bar{1}$ (No. 2)	$P\bar{1}$ (No. 2)
a (Å)	13.574(2)	9.81209(1)	10.830(1)	9.7938(5)
b (Å)	12.153(2)	10.726(1)	13.400(1)	10.7410(5)
c (Å)	10.029(3)	14.272(1)	13.826(1)	14.2759(7)
α (deg)	108.52(3)	104.834(2)	64.702(1)	104.962(1)
β (deg)	100.65(3)	101.034(2)	78.248(2)	100.945(1)
γ (deg)	108.52(3)	99.824(2)	83.552(2)	99.911(1)
V (Å^3)	1454.73(11)	1386.44(16)	1775.3(2)	1385.20(12)
Z	1	1	1	1
T (°C)	25(2)	−176(2)	−177(2)	−178(2)
λ (Å)	1.54178	0.71073	0.71073	0.71073
D_{calcd} (g cm^{-3})	1.034	1.241	1.197	1.397
μ (mm^{-1})	0.812	1.966	1.146	2.287
$R(F)$[b]	Rp = 5.08	0.0269	0.0256	0.0182
$R_w(F)$[c]	Rwp = 7.05	0.0666	0.0631	0.0461

[a] Powder diffraction data; $R_p = [\sum_i|y_{oi} - y_{ci}|/\sum|y_{oi}|]$; $R_{wp} = [\sum_i(w_i(y_{oi} - y_{ci})^2)/(\sum_i(w_iy_{oi})^2]^{1/2}$. [b] $R(F) = \sum||F_o| - |F_c||/\sum|F_o|$. [c] $R_w(F) = [\sum w(F_o^2 - F_c^2)^2/\sum w(F_o^2)^2]^{1/2}$.

Table 2. Selected Bond Lengths (Å) and Angles (deg) for **2**−**4** and **8**

	8[12]		**2**		**4**		**3**	
				Bond Lengths				
M(1)−N(11)	2.404(6)	*1.324*	2.514(2)	*1.254*	2.518(1)	*1.268*	2.724(2)	*1.254*
M(1)−N(12)	2.378(5)	*1.198*	2.473(2)	*1.213*	2.473(1)	*1.223*	2.660(2)	*1.190*
M(1)−N(21)	2.494(8)	*1.418*	2.786(2)	*1.526*	2.783(1)	*1.533*	2.986(2)	*1.516*
M(1)−N(22)	2.529(7)	*1.449*	2.793(2)	*1.533*	2.792(1)	*1.542*	2.922(2)	*1.452*
M(1)−C(23)	3.324	*2.244*	2.977(1)	*1.717*	2.956(2)	*1.706*	3.251(2)	*1.781*
M(1)−C(24)	3.640	*2.560*	3.085(2)	*1.825*	3.051(2)	*1.801*	3.499(2)[b]	*2.029*[b]
M(1)−C(25)	3.219	*2.139*	2.966(2)	*1.706*	2.942(2)	*1.692*	3.336(2)	*1.866*
M(1)−N(21)#1[c]	2.563(8)	*1.483*	2.610(1)	*1.350*	2.616(1)	*1.366*	2.813(2)	*1.343*
M(1)−N(22)#1[c]	2.641(9)	*1.561*	2.550(1)	*1.290*	2.552(1)	*1.302*	2.801(2)	*1.331*
M(1)−O(31)	2.437(9)	*1.357*	2.567(1)	*1.307*	2.583(1)	*1.333*	2.771(2)	*1.302*
M(1)−O(41)							2.781(1)	*1.311*
				Bond Angles				
N(11)−M(1)−N(12)	33.8(3)		32.34(4)		32.35(5)		29.78(5)	
N(21)−M(1)−N(22)	32.9(2)		28.87(3)		28.93(4)		27.22(4)	
N(21)#1[c]−M(1)−N(22)#1[c]	31.6(2)		31.25(4)		31.24(4)		28.71(4)	
O(30)−M(1)−O(40)							69.39(5)	

[a] Values in italics are corrected for the ionic radii (CN = 7, Yb^{2+} = 1.08 Å; CN = 8, Sr^{2+} = 1.26 Å, Eu^{2+} = 1.25 Å; CN = 9, Ba^{2+} = 1.47 Å).[13] [b] Indicates close contact. [c] #1 symmetry generated $-x + 1, -y + 1, -z + 1$ for **2** and **4** and $-x + 2, -y + 2, -z + 1$ for **8** and **3**.

pyrazolates and framed by terminal η^2-pyrazolates. The narrow bite angles (N−M−N = 28.87−32.35°) of the ligands are consistent with η^2-chelation of the formally eight-coordinate metal centers, along with fairly symmetrical bonding (Δ_{M-N} = 0.007−0.064 Å) of the pyrazolate ligands, which is in close agreement with other structurally characterized pyrazolates.[8b,c,9,12,14] Alternatively, to simplify the description of the coordination environment around the metal center, the metal coordination on the pyrazolate may be considered as one, as justified by the narrow N−M−N angle [N−N(cen)−Sr = 2.394 and 2.484 Å; N−N(cen)−Eu = 2.395 and 2.488 Å; (cen) = centroid of the N−N bond]. Moreover, metal bonding to the η^5-bonded pyrazolate rings is considered through the center of the five-membered ring (pz−Sr = 2.679 Å; pz−Eu = 2.659 Å; pz = centroid of bridging pyrazolate ring). One additional THF molecule [Sr−O = 2.567(2) Å; Eu−O = 2.583(1) Å; pz−M−O = 142.08° (**2**) and 141.96° (**4**)] completes the metal coordination sphere and leads to an overall distorted tetrahedral arrangement of the ligands around the metal, nicely visualizing the high steric demand of the π-bonded pyrazolate ligand (angles to all ligands from centroids = 100.42−142.08°). In addition, angles between the THF donor and the σ-bonded pyrazolate ligands range from 85.20° to 87.12°, whereas the angle between the η^2-pyrazolates is significantly larger (134.36°, **2**; 133.18°, **4**) because of steric interactions of the *tert*-butyl substituents. The resulting large voids in the metal coordination sphere are compensated for by close H−M contacts involving one *tert*-butyl group (C253−H25D) of the η^5-pyrazolate (H−Sr = 2.937 Å; H−Eu = 2.910 Å) and the THF donor (C31−H31A) (H−Sr = 2.937 Å; H−Eu = 2.960 Å). These distances lie well within the sum of the van der Waals radii of the metal and hydrogen (3.395−3.551 Å; Sr = 2.151 Å, Eu = 1.995 Å, H = 1.4 Å)[15] and thus can be considered a significant contribution toward the shielding of the metal centers. The overall M−N bond lengths increase from the terminal η^2-ligand (2.473−2.518 Å) through the bridging η^2-ligand (2.550−2.616 Å) to the tilted π-bonded

(14) Deacon, G. B.; Gitlits, A.; Roesky, P. W.; Bürgstein, M. R.; Lim, K. C.; Skelton, B. W.; White, A. H. *Chem.—Eur. J.* **2001**, *7*, 127.

(15) Hollemann, A. F.; Wiberg, E. *Lehrbuch der Anorganischen Chemie*, 101st ed.; de Gruyter: Berlin, 1995.

pyrazolate (2.783−2.793 Å), as expected from the increase in the number of metal−ligand contact sites.

However, the two bridging pyrazolates are almost coplanar with the M(1), N(21A), and N(22A) plane and the symmetry-equivalent M(1A), N(21), and N(22) plane [1.9(1)°, **2**; 3.6(1)°, **4**], confirming σ-η^2 coordination, whereas the M(1)−pz vector intersects the pyrazolate ring plane at angles close to the ideal 90° for π bonding (82.32°, **2**; 82.25°, **4**). The additional M−C contacts [2.942(2)−3.085(2) Å] are well within the sum of the van der Waals radii of the metal and an aromatic ring (3.725−3.881 Å; Ph = 1.73 Å)[15,16] and are comparable to those observed for π-η^5-pyrazolates in the homoleptic analogues **6** and [{Eu(*t*Bu$_2$pz)$_2$}$_4$] (**10**) (M−C = 3.029(7)−3.381(9) Å, **6**; 3.03(2)−3.32(2) Å, **10**).[9,14] Interestingly, the increase in the metal radius from Yb/Ca to Sr/Eu (Yb^{2+} = 1.14 Å; Ca^{2+} = 1.12 Å; Sr^{2+} = 1.26 Å; Eu^{2+} = 1.25 Å; CN = 8)[13] results in an increase in the coordination number by tilting of the μ-η^2:η^2-bridging pyrazolates in **8**, which could also be regarded as weakly μ-η^2:η^4, to the π-bonded μ-η^2:η^5-bridging ligands in **2**−**4**, or even higher if additional agostic M···H interactions are considered.

The molecular structure of **3** depicts bonding modes similar to those described above for **2** and **4**, although the larger ionic radius of barium (Ba^{2+} = 1.47 Å)[13] compared with the lighter metal analogues requires coordination of two THF cosolvents [Ba−O = 2.771(2) and 2.781(1) Å] to saturate the metal coordination sphere, giving a formal coordination number of 9. As described for **2** and **4**, the η^2-pyrazolates can be considered as monodentate ligands [N−N(cen)−Ba = 2.984 and 2.602 Å] because of their narrow bite angles (N−M−N = 27.22−29.78°), resulting in a distorted trigonal-bipyramidal arrangement with pyrazolate in the equatorial plane along with one THF donor (cen−Ba−cen = 133.75°; O−Ba−cen = 97.04−112.48°). The center of the η^5-bonded pyrazolate ring (pz−Ba = 2.984 Å; pz = centroid of the bridging pyrazolate ring) and the second THF molecule coordinate via the axial positions (pz−Ba−O = 169.29°). Once more, the larger angle between the pyrazolate ligands compared to the THF donors demonstrates the steric demand implemented by the *tert*-butyl substituents of the heterocyclic ring. However, the presence of the additional THF donor in lieu of agostic interactions does not result in a distortion of the symmetrical η^2-pyrazolate coordination (Δ_{Ba-N} = 0.012−0.064 Å) but leads to a larger inclination angle of the bridging μ-η^2:η^5-pyrazolate [Ba(1)−pz(cen) vector intersecting the ring plane at 105.5°], as well as surprisingly shorter Ba−N contacts (max 0.08 Å) than those in **2** and **4** (corrected for the metal radius). As a result, metal−carbon π bonding involving C(23) and C(25) is marginally weaker (0.07−0.16 Å, corrected for the metal radius; see Table 2) than that in **2** and **4** and substantially elongated for C(24) (0.20; 0.23 Å longer, corrected for the metal radius). The Ba(1)−C(24) contact [3.499(2) Å] still lies within the sum of the van der Waals radii of the metal and aromatic ring (3.97 Å; Ba = 2.24 Å), but it is probably better discussed as a weak bonding interaction. Apart from this contact, Ba(1)−C(23,25) bonds are in the range [3.10(1)−3.39(1) Å] of the hexanuclear **7**.[9] This structural trend is in contrast to the linear, homoleptic analogues **5**−**7,** where an increase in π bonding is observed for the heavier metals to satisfy the coordination sphere.[9] Nevertheless, an increase in the coordination number by additional Lewis base donors such as THF is commonly favored over an increase in the π bonding of the pyrazolate ligand, as seen in the formation of monomeric **9a**−**c** and the dinuclear structures **1**−**4**.[11]

The molecular structures of complexes **1**−**4** vividly illustrate the preference for terminal η^2 chelation of the pyrazolate ligand for the large, highly electropositive s and f block metals due to maximum overlap between the nitrogen sp^2 orbitals and the metal.[8,17] In monomeric complexes, as are frequently observed in the presence of Lewis donors, η^2 coordination is observed exclusively [cf. **9a**−**f**,[11] [M(Ph$_2$-pz)$_2$(DME)$_2$] (M = Yb, Eu, Sm),[18] [M(*t*Bu$_2$pz)$_2$(D)$_n$] (M = Ca, Sr, Ba; D = *N*,*N*,*N*′,*N*′-tetramethylethylenediamine, *N*,*N*,*N*′,*N*′,*N*″-pentamethyldiethylenetriamine, glyme, triglyme, tetraglyme)].[8b,c] Conversely, the absence or reduction of the number of available coligands leads to aggregation and more complex binding modes, typically involving the π system of the ligand core, as seen in **1**−**7**,[5−7,9] [{Yb(*t*Bu$_2$-pz)$_2$(THF)}$_2$] (**8**),[12] and [{Eu(*t*Bu$_2$pz)$_2$}$_4$] (**10**),[14] highlighting the diazacyclopentadienide character of the pyrazolate ligand. The μ-η^2:η^5-bridging mode of pyrazolate ligands has now been observed in a number of complexes (e.g., **5**−**7**,[9] **10**,[14] and [Ba$_6$(Me$_2$pz)$_8$(THF)$_6${(OSiMe$_2$)$_2$O}$_2$][19]) and seems to be preferred if no additional donors are present or capable of coordination for steric reasons. Another example of the particular stability of the bridging μ-η^2:η^5-pyrazolate structural motif has recently been demonstrated by Winter and co-workers for mixed-ligand pyrazolate complexes of the heavy alkaline-earth metals, namely, [(η^2-*t*Bu$_2$pz)Ca(μ-η^5:η^2)(μ-η^2:η^5)-*t*Bu$_2$pz)(μ-η^5:η^2-*t*Bu$_2$pz)Ca(π^5-L*t*Bu)] (**11a**) and [M(μ-η^5:η^2-*t*Bu$_2$pz)(π^5-L*t*Bu)]$_2$ (M = Sr, **11b**; Ba, **11c**) [L*t*BuH = *N*-*tert*-butyl-4-(*tert*-butylimino)-2-penten-2-amine]. Furthermore, the efficiency and flexibility of shielding the metal centers by μ-η^2:η^5-bridging pyrazolates is demonstrated upon comparing the π-η^5-bridging pyrazolates in **3** with the hexanuclear **7**, despite the presence of two THF donors in **3**. The additional coordination only leads to a slight decrease in the tilt angle of the bridging pyrazolates, implying weaker metal−ligand π interactions, whereas in **11c**, the bridging ligands are much more inclined toward the metal center to compensate for the missing donor, resulting in longer and more asymmetric Ba−N distances (Table 3).[17]

The detailed analysis of bonding trends within the group of alkaline-earth metals becomes possible when considering [{Mg(*t*Bu$_2$pz)$_2$(THF)}$_2$] and [{Mg(*t*Bu$_2$pz)$_2$}$_2$] as the lighter analogues[8a] of the alkaline-earth metal series **1**−**3** and **5**−**7**.[9] The small diameter of the magnesium metal center leads to

(16) Pauling, L. *The Nature of the Chemical Bond*, 3rd ed.; Cornell University Press: Ithaca, NY, 1960.

(17) El-Kaderi, H.; Heeg, M. J.; Winter, C. H. *Eur. J. Inorg. Chem.* **2005**, 2081.

(18) Deacon, G. B.; Delbridge, E. E.; Skelton, B. W.; White, A. H. *Eur. J. Inorg. Chem.* **1999**, 751.

(19) Steiner, A.; Lawson, G. T.; Walfort, B.; Leusser, D.; Stalke, D. *J. Chem. Soc., Dalton Trans.* **2001**, 219.

Table 3. Comparison of Pyrazolato Metal−Nitrogen Distances [Å] and Angles [deg] in **2** and **3** with Those of **11b**,**c**[17]

	M−N (η^2)	M−N (π)	M−pz(cen)−pz
2	2.610(1)	2.786(2)	80.1
	2.550(1)	2.792(2)	
11b	2.614(5)	2.855(4)	80.9
	2.618(4)	2.897(4)	
3	2.813(2)	2.986(2)	79.3
	2.801(2)	2.992(2)	
11c	2.776(6)	3.004(6)	80.9
	2.793(6)	3.036(6)	

dinuclear structures with μ-η^1:η^1 bridging ligands, but already the larger calcium (assuming analogous bonding to **8** vide infra) exhibits μ-η^2:η^2 chelation. Upon descending Group 2, more extensive π bonding of the pyrazolate core is observed, also seen in the homoleptic analogues **5**−**7** and **10** ([{M(*t*Bu$_2$pz)$_2$}$_n$] where n = 2 (Mg), 3 (Ca), 4 (Sr/Eu), 6 (Ba)), where the linear chain length increases with the ionic radius of the metal.[9,14] Considering the very similar ionic radii (Sr^{2+} = 1.26 Å; Eu^{2+} = 1.25 Å; CN = 8)[13] and the isostructural, homoleptic analogues **6** and **10**, it is not surprising that **2** and **4** display identical metal−ligand bonding within experimental error.[9,14] In addition, the similar IR spectroscopic data (especially of **2** and **4)** further underline the close structural relationship between divalent lanthanoids and alkaline-earth metals.[9,20] The series of compounds presented herein provides additional affirmation regarding the likelihood of identical bonding, as is observed on the basis of powder X-ray data for the calcium compound **1** and the respective ytterbium species **8**, on the basis of similar ionic radii (Ca^{2+} = 1.12 Å; Yb^{2+} = 1.14 Å; CN = 8).[13]

Thermogravimetric Analysis (TGA) and Sublimation Studies. Compounds **1**−**3** and **5**−**7** were studied by TGA (under 1 atm of nitrogen flow) and sublimation to test their suitability as CVD precursors. The direct comparison of the thermal properties of the solvated and donor-free species allows a rare insight into the influence of the cosolvent on associated thermal properties. TGA (Figure 3a) showed that loss of donors in compounds **1**−**3** begins prior to 150 °C and **1**−**3** finish their significant weight loss prior to 194, 335, and 423 °C, respectively. Further heating to 600 °C only slightly reduces the remaining residue to 17.3, 20.6, and 35.7 wt % of the initial content (**1**−**3**, respectively). Comparatively, the homoleptic compounds **5**−**7** exhibit significant weight loss prior to 394, 238, and 436 °C with residues of 16.6, 25.6, and 40.3%, respectively. Notably, the strontium tetranuclear **6** loses weight more rapidly than the calcium trinuclear **5**, but more residue is left behind. Analysis of the metal content of the residues from **5**−**7** by inductively coupled plasma (ICP) measurements revealed that nearly all of the metal, 97−99% for **5**−**7**, respectively, remained in the residue. Despite the initial expectation that polynuclear **5**−**7** should exhibit some volatility because a small degree of mass transport had been observed during preparation by high-temperature direct metalation (250 °C) under vacuum from excess metal and pyrazole,[9] it becomes clear that changes in the conditions, such as dynamic vacuum, as used in the sublimation studies, ambient pressure as applied in TGA experiments, or sealed tube as used during preparation, play a major role.

As representatives, compounds **1** and **6** were each heated to 300 °C at 26 mTorr in a vertical sublimator with a dry-ice-cooled coldfinger. For **1**, minimal amounts of calcium were retrieved from a white powder that collected on the coldfinger. Analysis of the white powder by NMR spectroscopy revealed the presence of both *t*Bu$_2$pzH and a small amount of calcium pyrazolate. Analysis of the powder for metal content showed that only 1.4 ± 0.1 wt % of the powder was calcium. A similar analysis for **6** showed that the white powder collected on the coldfinger contained pyrazolate and *t*Bu$_2$pzH and 7.12 ± 0.06 wt % of strontium. These results suggest that some form of [Sr(*t*Bu$_2$pz)$_2$]$_n$ sublimed along with decomposition and consequent liberation of the free ligand. The differences in metal transport between **1** and **6** suggest that the decomposition is likely enhanced by the presence of THF. Likewise, TGA of **9a**−**f** revealed liberation of the neutral coligand, followed by pyrazole.[11] Winter and coworkers recently reported on related compounds containing polyether and polyamine donors that decompose in a horizontal sublimation apparatus to yield donor and free ligands.[8c] This indicates that the combination of ethers, amine donors, and pyrazolate ligands is not effective enough to afford sufficient thermal stability of alkaline-earth pyrazolate compounds for sublimation.

A promising alternative to the ethereal and amine donors is provided by complexes previously reported by our group.[11] Replacing the traditional neutral donors, such as THF, with the free pyrazole ligand, as shown with the monomeric compounds [M(3,5-Me$_2$pz)$_2$(3,5-Me$_2$pzH)$_4$] (M = Ca, Sr) (**12a**,**b**), results in dramatically improved thermal stability. While each of **12a** and **12b** exhibits loss of the dative ligand in TGA (Figure 3b), sublimation of [Ca(3,5-Me$_2$pz)$_2$(3,5-Me$_2$pzH)$_4$] (**12a**) at the above conditions showed improved metal transport in the vapor phase. Thus, the white powder collected on the coldfinger contained 14.2 wt % of calcium, a larger percentage than was found in **12a** itself. While this does not indicate the sublimation of the intact complex, it strongly suggests that a partially decomplexed aggregate with an intact metal−pyrazolate core was transported into the vapor phase, in contrast to the behavior of ethereal and amine-containing compounds. Current technology frequently relies on the addition of excess free ligand, as was used in the CVD of alkaline-earth metal β-diketonate CVD precursors.[21] Further alternatives take advantage of the solubility of the oligonuclear complexes, making them candidates for aerosol-assisted CVD, for which oligonuclear barium β-diketonates have found success.[22]

Summary

This work compares the structural and thermal properties of a series of 3,5-di-*tert*-butylpyrazolates. Donor-free and donor-containing polymeric and dinuclear species were

(20) Harder, S. *Angew. Chem., Int. Ed.* **2004**, *43*, 2714; *Angew. Chem.* **2004**, *116*, 2768.

(21) (a) Hubert-Pfalzgraf, L. G. *Appl. Organomet. Chem.* **1992**, *6*, 627. (b) Turnipseed, S. B.; Barkley, R. M.; Sievers, R. E. *Inorg. Chem.* **1991**, *30*, 1164.

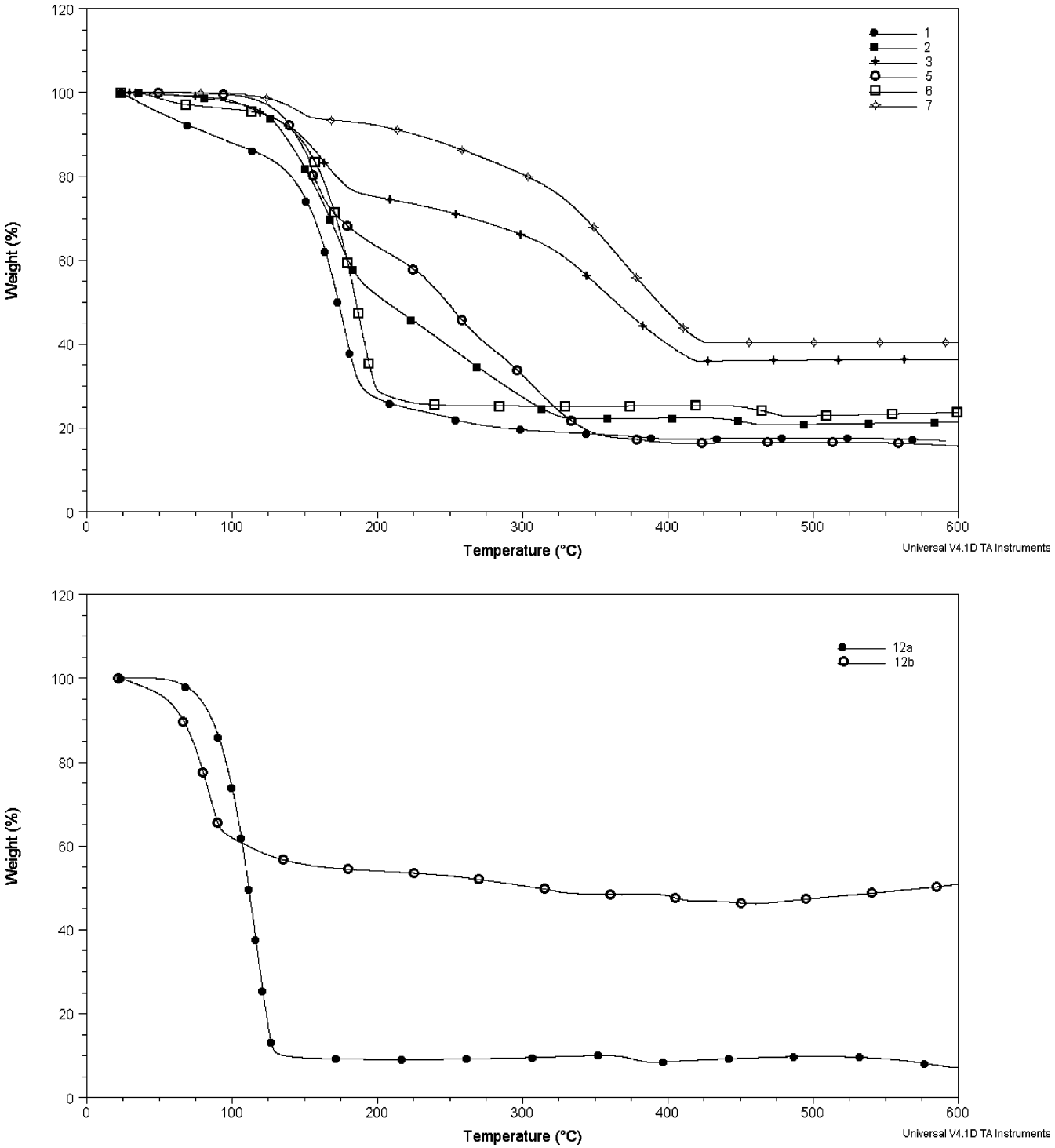

Figure 3. TGA patterns of complexes (a) **1**−**3**, **5**−**7**, and (b) **12a**,**b** under nitrogen with a temperature ramp of 10 °C min^{-1}.

compared to analyze the role of the donor. In the presence of THF, dinuclear molecules with μ-η^2:η^n-chelating pyrazolates to achieve coordinative saturation are obtained. The bonding modes observed in **1**−**4** [Ca (μ-η^2:η^2), Sr/Eu (μ-η^2:η^5), Ba (μ-η^2:η^5)] are similar to, but less complex than, those in the homoleptic analogues **5**−**7** and **10**.[9,14] Bridging pyrazolate fragments [M_2(μ-η^2:η^5-*t*Bu_2pz)$_2$] (M = Ca, Sr, Ba) have also been observed in related compounds (**5**−**7** and **11a**−**c**) and indicate their exceptional stability and ability to coordinatively saturate the metal centers.[9,17] A comparison of the volatility and thermal stability of the heteroleptic, dinuclear pyrazolate complexes **1**−**3** with the homoleptic oligonuclear complexes **5**−**7** suggests that the presence of ethereal neutral donors may promote decomposition through close contacts, but further studies are needed to support this view. An alternative neutral coligand, such as the free pyrazole, is a promising alternative. It appears that secondary interactions, including hydrogen and π bonding, as well as

(22) Hubert-Pfalzgraf, L. G.; Guillon, H. *Appl. Organomet. Chem.* **1998**, *12*, 221.

agostics are small but important contributors toward the coordinative saturation.[9,11] The small contributions become significant in light of the relatively weak metal−ligand/donor bonds. However, their role needs to be evaluated further to establish if these interactions can provide the necessary thermal stability required for high-performance CVD precursors.

Experimental Section

General Considerations. All compounds described herein are air- and moisture-sensitive and were synthesized under an inert gas atmosphere (purified nitrogen or argon) utilizing standard Schlenk-line and glovebox techniques.[23] Tetrahydrofuran (THF) and hexane were freshly distilled under nitrogen from a sodium/potassium alloy and acetonitrile from P_2O_5 and degassed in three freeze−pump−thaw cycles. Liquid ammonia was dried by treatment with sodium prior to condensation into the dry-ice-cooled reaction vessel. The alkaline-earth metals were of commercial standard +99.9% (calcium turnings, strontium granules, barium granules, and europium-distilled ingots stored under oil). 3,5-Di-*tert*-butylpyrazole was synthesized via a modified literature procedure,[24] and compounds **5**−**7** were prepared as described previously.[9]

IR data (4000−650 cm^{-1}) were obtained for mineral oil mulls sandwiched between NaCl plates with a Perkin-Elmer Paragon FTIR spectrometer. ^1H and $^{13}C\{^1H\}$ NMR spectra were recorded on a Bruker Avance spectrometer (300 MHz, 25 °C) unless indicated otherwise, and the chemical shifts were referenced to the residual solvent signals. NMR solvents were dried over calcium hydride (benzene-d_6) or used as received in small ampules (toluene-d_8 and THF-d_8). Melting points were obtained in capillaries sealed under nitrogen and are uncalibrated. MS spectra were obtained for solutions in acetonitrile sandwiched between pure solvent with a Micromass Platform II electrospray source and a Harvard apparatus syringe pump. TGA experiments were conducted on a Universal V3.4C TA Instrument, Auto TGA 2950HR V5.4A, and ICP measurements were performed on a Perkin-Elmer Optima 3300 DV ICP optical emission spectrometer. Elemental analyses were obtained with elemental analysis Vario EL from Elementar Analysensysteme GmbH, located at TU Graz, Austria.

Preparation of Compounds 1, 1a, and 2-4. Bis(3,5-di-*tert*-butylpyrazolato)bis(tetrahydrofuran)calcium (1a) and Bis[bis-(3,5-di-*tert*-butylpyrazolato)(tetrahydrofuran)calcium] (1). (a) 1 and 1a by the Addition of THF to 5. A sample of **5** (0.20 g, 0.18 mmol) was dissolved in THF (20 mL) and the solvent subsequently removed in vacuo, resulting in a white solid **1a** [0.25 g, 0.46 mmol (85%)]. ^1H NMR (300 MHz, benzene-d_6, 25 °C): δ 6.15 (s, 2H, H4−pz), 3.48 (s, 8H, α-THF), 1.44 (s, 36H, *t*Bu), 1.32 (s, 8H, β-THF). Recrystallization of **1a** from hexane afforded **1**. Because of the small-scale experiment, no melting point and IR data are available for **1a**, but ^1H NMR data allowed a clear assignment of ligand/coligand stoichiometry. Analytical data for compound **1** prepared by the addition of THF to **5** are identical with those of compound **1** prepared by direct metalation (below). ^1H NMR data of **5** in THF-d_8 are consistent with those of **1a** in benzene-d_6, considering the solvent effect leading to the formation of monomeric species in the presence of excess donor solvent (here THF-d_8).

^1H NMR (300 MHz, THF-d_8, 25 °C) of **5**: δ 5.78 (s, 2H, H4−pz), 1.29 (s, 36H, *t*Bu). ^{13}C NMR of **5**: δ 145.5 (*ipso*-*C*(Ph)), 97.0 (*C*H(pz)), 32.2 (*C*CH_3), 30.8 (C*C*H_3).

(b) 1 by Direct Metalation in Liquid Ammonia. Calcium metal (0.08 g, 2.0 mmol) and 3,5-di-*tert*-butylpyrazole (0.72 g, 4.0 mmol) were dispersed in THF (30 mL), anhydrous ammonia (30 mL) was condensed into the Schlenk flask, and the reaction mixture was subsequently allowed to warm to room temperature while stirring overnight. The solvent was removed in vacuo and the residue dissolved in hexane (20 mL). The resulting liquid was filtered through a filter frit layered with Celite, concentrated, and stored at −20 °C. White, soft crystals of **1** appeared overnight and were analyzed by X-ray powder diffraction [0.84 g (89%)]. Mp: 165−167 °C. ^1H NMR (300 MHz, benzene-d_6, 25 °C): δ 6.16 (s, 4H, H4−pz), 3.22 (q, 8H, α-THF), 1.47 (s, 72H, *t*Bu), 1.15 (q, 8H, β-THF). ^{13}C NMR: δ 164.9 (*ipso*-*C*(*t*Bu)), 99.9 (*C*H(pz)), 68.9 (α-THF), 32.8 (*C*CH_3), 32.2 (C*C*H_3), 25.4 (β-THF). IR (Nujol): 3190 (w), 3116 (m), 1926 (w), 1755 (w), 1589 (m), 1560 (m), 1503 (s), 1405 (s), 1358 (m), 1318 (m), 1296 (m), 1252 (s), 1220 (s), 1099 (s), 1038 (s), 996 (s), 914 (m), 886 (s), 801 (s), 783 (s), 725 (m), 669 (m) cm^{-1}. MS (80 eV, ES): *m*/*z* (%) 521.3 (5) $[Ca(tBu_2pz)_2(MeCN)_3]^+$, 481.6 (5) $[Ca(tBu_2pz)(tBu_2pzH)(MeCN)_2]^+$, 425.6 (55) $[Ca(tBu_2pz)(tBu_2pzH)(MeCN)_2C_4H_8]^+$, 423.5 (95) $[Ca(tBu_2pz)(tBu_2pzH)(MeCN)_2C_4H_{10}]^+$, 286.3 (35) $[Ca(tBu_2pz)(MeCN)_3C_4H_{10}]^+$, 284.4 (35) $[Ca(tBu_2pz)(MeCN)_3C_4H_8]^+$, 222.4 (100) $[HtBu_2pzH(MeCN)]^+$.

Bis[bis(3,5-di-*tert*-butylpyrazolato)(tetrahydrofuran)strontium] (2). (a) 2 by the Addition of THF to 6. A sample of **6** (0.15 g, 0.08 mmol) was dissolved in THF (20 mL), and the solvent was removed in vacuo, leaving behind a white solid **2** [0.12 g, 0.24 mmol (75%)]. ^1H NMR (300 MHz, benzene-d_6, 25 °C): δ 6.25 (s, 4H, H4−pz), 3.31 (t, 8H, α-THF), 1.45 (m, 72H, *t*Bu), 1.19 (t, 8H, β-THF). ^{13}C NMR: δ 164.9 (*ipso*-*C*(*t*Bu)), 99.9 (*C*H(pz)), 68.9 (α-THF), 32.8 (*C*CH_3), 32.2 (C*C*H_3), 25.4 (β-THF). A small amount of free ligand identified in the NMR spectrum, together with a small excess of THF, suggested a small degree of hydrolysis, a common observation upon working on such a small scale. The identity of **2** (with correct integration) was further confirmed in the product of direct metalation (see below). ^1H NMR data of **6** in THF-d_8 are consistent with those of **2** in benzene-d_6, considering the solvent effect leading to the formation of monomeric species in the presence of excess donor solvent (here THF-d_8).

^1H NMR (300 MHz, THF-d_8, 25 °C) of **6**: δ 5.79 (s, 2H, H4−pz), 1.29 (s, 36H, *t*Bu). ^{13}C NMR of **6**: δ 159.1 (*ipso*-*C*(Ph)), 96.7 (*C*H(pz)), 32.7 (*C*CH_3), 32.4 (C*C*H_3).

(b) 2 by Direct Metalation in Liquid Ammonia. In a procedure analogous to the preparation of **1**, strontium metal (0.17 g, 2.0 mmol), 3,5-di-*tert*-butylpyrazole (0.72 g, 4.0 mmol), THF (30 mL), and liquid ammonia (30 mL) afforded **2** after evaporation of the solvent and recrystallization from hexane (30 mL) by cooling to −20 °C in the form of colorless prisms [0.65 g (63%)]. Mp: 340−346 °C. ^1H NMR (300 MHz, benzene-d_6, 25 °C): δ 6.25 (s, 4H, H4−pz), 3.29 (t, 8H, α-THF), 1.46 (d, 72H, *t*Bu), 1.16 (t, 8H, β-THF). ^{13}C NMR: δ 167.1 (*ipso*-C(*t*Bu)), 102.9 (*C*H(pz)), 68.4 (α-THF), 32.2 (*C*CH_3), 31.9 (C*C*H_3), 25.6 (β-THF). IR (Nujol): 3193 (w), 3113 (m), 1755 (w), 1592 (w), 1552 (s), 1497 (s), 1402 (m), 1357 (s), 1316 (m), 1306 (m), 1247 (s), 1220 (s), 1206 (s), 1099 (w), 1041 (s), 1010 (s), 996 (s), 917 (m), 890 (s), 798 (s), 776 (m), 735 (m) cm^{-1}. Elem anal. Calcd for $C_{52}H_{92}N_8O_2Sr_2$ (1036.58): C, 60.25; H, 8.95; N, 10.81. Found: C, 60.48; H, 9.08; N, 11.19.

Bis[bis(3,5-di-*tert*-butylpyrazolato)bis(tetrahydrofuran)barium] (3). (a) 3 by the Addition of THF to 7. A sample of **7** (0.22 g, 0.07 mmol) was dissolved in THF (20 mL), and the solvent was removed in vacuo, leaving behind a white solid **3** [0.25 g, 0.40 mmol (95%)]. ^1H NMR (300 MHz, benzene-d_6, 25 °C): δ 6.38−

(23) Shriver, D. F.; Drezdzon, M. A. *The Manipulation of Air-Sensitive Compounds*, 2nd ed.; Wiley: New York, 1986.
(24) Elguero, J.; Gonzalez, E.; Jacquier, R. *Bull. Soc. Chim. Fr.* **1968**, 707.

6.15 (m, 4H, H4−pz), 3.56 (s, 32H, α-THF), 1.42−1.31 (m, 176H, *t*Bu and *β*-THF). ^{1}H NMR data of **7** in THF-d_8 are consistent with those of **3** in benzene-d_6, considering the solvent effect leading to the formation of monomeric species in the presence of excess donor solvent (here THF-d_8).

^{1}H NMR (300 MHz, THF-d_8, 25 °C) of **7**: δ 5.81 (s, 2H, C4−H(pz)), 1.26 (s, 36H, *t*Bu-H)). ^{13}C NMR of **7**: δ 158.7 (*ipso*-*C*(pz)), 96.7 (*C*H(pz)), 32.8 (*C*CH$_3$), 32.4 (C*C*H$_3$).

(b) 3·THF by Direct Metalation in Liquid Ammonia. In a fashion similar to that of **1** and **2**, barium (0.27 g, 2 mmol), 3,5-di-*tert*-butylpyrazole (0.72 g, 4 mmol), THF (30 mL), and liquid ammonia (30 mL) were reacted to yield **3**·THF after recrystallization from hot THF (5 mL)/hexane (10 mL) as colorless blocks at room temperature [0.60 g (45%)]. Mp: >350 °C. ^{1}H NMR (300 MHz, benzene-d_6, 25 °C): δ 6.22 (s, 4H, H4−pz), 3.53 (s, 20H, α-THF), 1.37 (m, 92H, *t*Bu + *β*-THF). ^{13}C NMR: δ 163.9 (*ipso*-*C*(Ph)), 103.4 (*C*H(pz)), 68.2 (α-THF), 32.8 (*C*CH$_3$), 32.1 (C*C*H$_3$), 26.1 (*β*-THF). IR (Nujol): 3184 (w), 3111 (m), 1754 (w), 1572 (w), 1552 (s), 1497 (s), 1399 (s), 1358 (s), 1304 (m), 1247 (s), 1215 (s), 1073 (m), 1039 (s), 1006 (s), 916 (s), 882 (s), 789 (s), 662 (m) cm^{-1}. Elem anal. Calcd for [Ba$_2$(*t*Bu$_2$pz)$_4$(THF)] $C_{48}H_{84}Ba_2N_8O_1$ (1063.88): C, 54.19; H, 7.96; N, 10.53. Found: C, 52.45; H, 8.01; N, 10.20. This indicated partial loss of THF.

Bis[bis(3,5-di-*tert*-butylpyrazolato)(tetrahydrofuran)europium] (4) by Direct Metalation. Analogous to the preparation of **2**, europium metal (0.33 g, 2.0 mmol), 3,5-di-*tert*-butylpyrazole (0.72 g, 4.0 mmol), THF (30 mL), and liquid ammonia (30 mL) afforded **4** after evaporation of the solvent, recrystallization from hot hexane (30 mL), and subsequent cooling to room temperature in the form of yellow rods [0.53 g (56%)]. Mp: 246 °C. Because of the strong paramagnetic nature of Eu^{2+}, NMR spectra could not be obtained. IR (Nujol): 3113 (m), 1754 (w), 1590 (m), 1556 (m), 1497 (s), 1399 (s), 1359 (s), 1309 (s), 1248 (s), 1218 (s), 1102 (m), 1036 (s), 997 (s), 916 (s), 887 (s), 797 (s), 779 (m), 728 (s), 664 (m) cm^{-1}. Elem anal. Calcd for $C_{52}H_{92}Eu_2N_8O_2$ (1165.268): C, 53.60; H, 7.96; N, 9.62. Found: C, 53.34; H, 8.03; N, 9.51.

Crystallography. Powder X-ray diffraction data were collected in Bragg−Brentano geometry on a Bruker AXS D8 Advance automated diffractometer equipped with a capillary stage using Cu Kα radiation (λ = 1.540 619 Å) and a focusing primary monochromator of the Johansson type. The crystalline powder of **1** was carefully packed in the glass capillary in the drybox and then placed in the sample holder. The step size was 0.02° in 2θ. The data were collected in four repeating runs with 0.2 increments in θ and refined as a structural phase using the DIFFRAC^{plus} software package.[25] A powder pattern was calculated based on data obtained for **8** from the Cambridge Structural Database. After replacement of ytterbium for calcium, the structure was refined. No additional peaks were detected, confirming the purity of the sample.

Single-crystal X-ray diffraction experiments for **2**−**4** were performed on a Bruker AXS SMART CCD system, complete with a three-circle goniometer using graphite-monochromated Mo Kα radiation (λ = 0.710 73 Å) and narrow (0.3° in θ) frame exposures. The crystals were obtained as mentioned above and mounted as described previously.[9] A hemisphere of data was collected for each sample at low temperature (see Table 1), and the cell parameters were refined using *SMART* and integrated with *SAINT* software package.[26] Absorption corrections were applied using *SADABS*, and the structure was solved and refined using *SHELXS-97* and *SHELXL-97*.[27] All non-hydrogen atoms were refined anisotropically and hydrogen atoms constrained using a riding model; *U*(H) was set as 1.2 times U_{eq} for the parent atom. In compound **3**, [{Ba(*t*Bu$_2$pz)$_2$(THF)$_2$}$_2$], a THF solvent molecule, was removed from refinement using *Platon* because of an unresolvable disorder.[28]

TGA and Sublimation Experiments. Samples of **1**−**3** and **5**−**7** (10−25 mg) were loaded in air onto platinum pans and were stable for the duration of the loading time. A flow of 100% nitrogen gas was sent over the balance at a rate of 44 mL/min, while the temperature was ramped from room temperature to 600 °C at a rate of 10 °C min^{-1}.

The metal contents of the residues remaining in the pans were measured using ICP analysis. The powdered residues were dissolved in known volumes of 10% aqueous nitric acid solutions. These solutions and a series of standard solutions of known calcium, strontium, and barium concentration were analyzed through ICP by measuring the intensities of spectral observations at 317.933 nm (calcium), 421 nm (strontium), and 455 nm (barium). The metal content in the residue was then calculated based on the intensities of the standards.

In a typical sublimation experiment, a sample (50−100 mg) was placed in the bottom of a vertical sublimator with a dry-ice-cooled finger and heated to 300 °C under a vacuum of 26 mTorr. The metal contents of the sublimate and the unsublimed residue were determined by dissolving mass samples in dilute nitric acid for ICP analysis. The sublimate was also analyzed by ^{1}H NMR.

Acknowledgment. We gratefully acknowledge support from the Monash University Small Grant Scheme, the Australian Research Council, and the National Science Foundation (Grant CHE-0108098 including a supplement and Grant CHE-0505863), enabling the collaboration between Monash University and Syracuse University. Purchase of the X-ray diffraction equipment was made possible with grants from the National Science Foundation (Grants CHE-9527858 and CHE-0234912), Syracuse University, and the W. M. Keck Foundation. We thank Dr. C. M. Forsyth at Monash University for collecting the mass spectrometry data, Prof. Frank Uhlig at TU Graz for providing us with the elemental analysis data, Dr. William T. Winter at SUNY ESF for use of his TGA instrument, and Dr. Deborah Kerwood (Syracuse University) for assistance with the variable-temperature NMR data.

Supporting Information Available: Figures S1−S4 displaying full experimental details for variable-temperature NMR studies, Tables S5−S19 listing structural data collection and refinement, atomic coordinates, bond lengths and angles, and thermal displacement parameters for **2**−**4**; Figure S20 and Table S21 showing powder diffraction data for **1**. This material is available free of charge via the Internet at http://pubs.acs.org.

IC061294D

(25) Bruker AXS Inc. *DIFFRAC^{plus}*, version 2.3; Karlsruhe, Germany, 2000.

(26) In *SMART and SAINT software for CCD diffractometers*; Bruker AXS Inc.: Madison, WI, 1997−2003.

(27) (a) Sheldrick, G. M. *SADABS: Program for Absorption Correction Using Area Detector Data*; University of Göttingen: Göttingen, Germany, 1996. (b) Sheldrick, G. M. *SHELXTL-Plus: Program Package for Structure Solution and Refinement*; Siemens: Madison, WI, 1999.

(28) Spek, A. L. *PLATON for Windows*; Utrecht University: Utrecht, The Netherlands, 2000.